ACS Catalysis

Review

pubs.acs.org/acscatalysis

Damage Management in Water-Oxidizing Catalysts: From Photosystem II to Nanosized Metal Oxides

Mohammad Mahdi Najafpour,*[,†,‡,△] Monika Fekete,[§,△] Davood Jafarian Sedigh,[†] Eva-Mari Aro,[∥] Robert Carpentier,[⊥] Julian J. Eaton-Rye,[#] Hiroshi Nishihara,[¶] Jian-Ren Shen,[□] Suleyman I. Allakhverdiev,*[,■,●,▲] and Leone Spiccia*[,§]

[†]Department of Chemistry, [‡]Center of Climate Change and Global Warming, Institute for Advanced Studies in Basic Sciences (IASBS), Zanjan 45137-66731, Iran

[§]School of Chemistry and the ARC Centre of Excellence for Electromaterials Science, Monash University, Victoria 3800, Australia

[∥]Department of Biochemistry and Food Chemistry, University of Turku, FI-20014 Turku, Finland

[⊥]Groupe de Recherche en Biologie Végétale (GRBV), Université du Québec à Trois-Rivières, C.P. 500, Trois-Rivières, Québec G9A 5H7, Canada

[#]Department of Biochemistry, University of Otago, P.O. Box 56, Dunedin 9054, New Zealand

[¶]Department of Chemistry, School of Science, The University of Tokyo, 7-3-1 Hongo, Bunkyo-ku, Tokyo 113-0033, Japan

[□]Photosynthesis Research Center, Graduate School of Natural Science and Technology/Faculty of Science, Okayama University, Okayama 700-8530, Japan

[■]Controlled Photobiosynthesis Laboratory, Institute of Plant Physiology, Russian Academy of Sciences, Botanicheskaya Street 35, Moscow 127276, Russia

[●]Institute of Basic Biological Problems, Russian Academy of Sciences, Pushchino, Moscow Region 142290, Russia

[▲]Department of Plant Physiology, Faculty of Biology, M. V. Lomonosov Moscow State University, Leninskie Gory 1-12, Moscow 119991, Russia

ABSTRACT: Current energy resources largely rely on fossil fuels that are expected to be depleted in 50−200 years. On a global scale, the intensive use of this energy source has resulted in highly detrimental effects to the environment. Hydrogen production by water splitting, with sunlight as the main energy source, is a promising way to augment the production of renewable energy; however, the development of an efficient and stable water-oxidizing catalyst remains a key task before a technological breakthrough based on water splitting can be realized. A main issue hampering the development of commercially viable, non-precious-metal-based catalysts is their susceptibility to degradation. To efficiently address this major drawback, self-healing catalysts that can repair their structure without human intervention will be necessary. In this review, we focus on water oxidation by natural and artificial Mn-, Co-, and Ni-based catalysts and then discuss the self-healing properties that contribute to sustaining their catalytic activity.

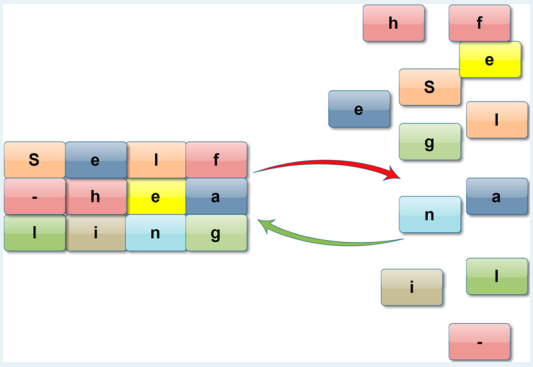

KEYWORDS: *water oxidation catalysts, self-healing catalysts, photosystem II, manganese, cobalt, nickel*

INTRODUCTION

Our overwhelming reliance on fossil fuels has resulted in devastating consequences that are causing global changes in our environment. These worldwide phenomena point to the emergence of major economic, social, and ecological problems, potentially in the near future, and for generations to come.[1] To mitigate this situation and also to address the depletion of fossils fuels, the implementation of new, clean sources of energy is urgently needed. Physical sources of green electricity, such as wind, tidal, geothermal, or photovoltaic energy, are all viable candidates. Developing efficient ways to store excess power, however, is essential to their successful integration into the power supply chain, since this energy will be provided intermittently. An additional and promising solution is artificial photosynthesis. In this process, the energy of solar irradiation is directly converted to chemical energy stored in chemical bonds as fuels.[1,2] Water splitting, powered entirely or in part by solar energy, can be utilized to produce H_2 as a green fuel (Figure 1 and eqs 1−3).

$$2H_2O \rightarrow 4H^+ + O_2 + 4e^- \quad E^0 = (1.23 - 0.059\ \mathrm{pH})\ \mathrm{V} \tag{1}$$

Received: October 2, 2014
Revised: December 15, 2014
Published: January 21, 2015

DOI: 10.1021/cs5015157
ACS Catal. 2015, 5, 1499−1512

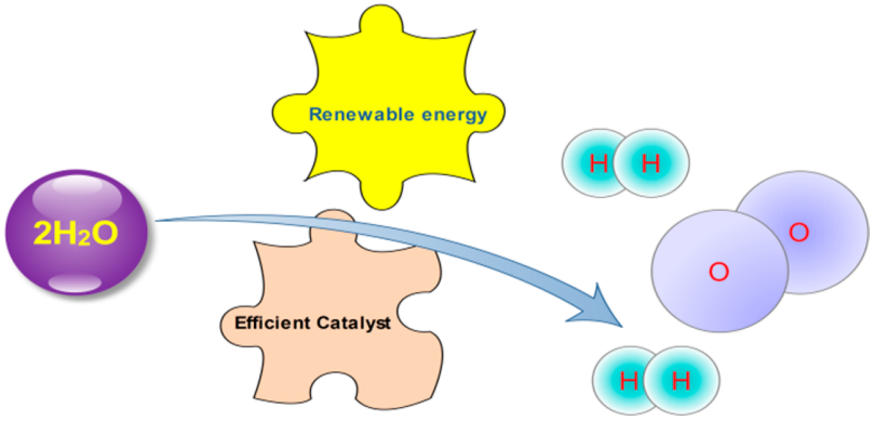

Figure 1. Hydrogen produced by water splitting is a viable way of storing energy available from various renewable sources.

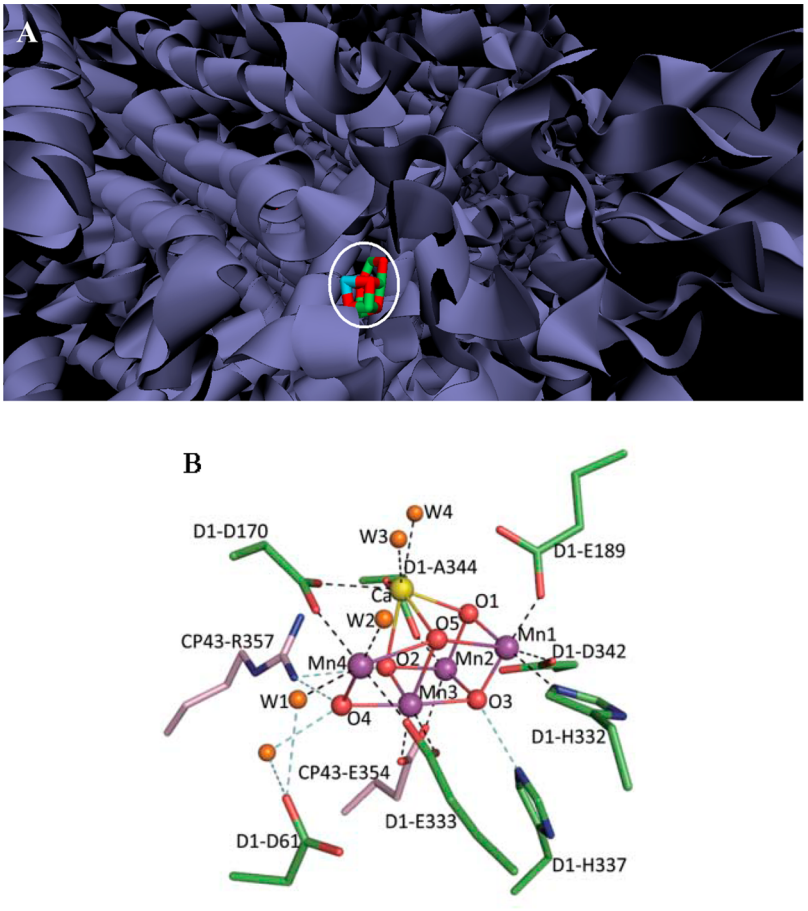

Figure 2. $CaMn_4O_5(H_2O)_4$ (Ca, blue; Mn, green; O, red) cluster (enclosed in white circle) and surrounding amino acids. Amino acid residues in photosystem II (PSII) are involved in proton, water, and oxygen transfer. The roles of the residues in direct contact with the Mn−Ca cluster include regulation of charges and electrochemistry of the $CaMn_4O_5(H_2O)_4$ cluster and assisting with the coordination of water molecules at appropriate metal sites and stabilization of this cluster. The image was made with Visual Molecular Dynamics (VMD), which is owned by the Theoretical and Computational Biophysics Group, NIH Resource for Macromolecular Modeling and Bioinformatics, at the Beckman Institute, University of Illinois at Urbana−Champaign. The original data is from ref 21 (PDB: 3ARC) (A). Schematic depiction of the $CaMn_4O_5(H_2O)_4$ cluster (B). Image B is reprinted with permission from ref 21. Copyright (2011) by Nature Publishing Group.

$$4H^+ + 4e^- \rightarrow 2H_2 \qquad E^0 = (0.00 - 0.059\ \mathrm{pH})\ \mathrm{V} \qquad (2)$$

$$2H_2O \rightarrow 2H_2 + O_2$$

$$\Delta E^0_{\mathrm{cell}} = 1.23\mathrm{V};\ \Delta G = 475\ \mathrm{kJ/mol} \qquad (3)$$

Water electrolysis is an endothermic reaction that requires external energy input to proceed. The thermodynamic and kinetic limitations of the water oxidation reaction (eq 1), involving multielectron transfer, are especially challenging to overcome and depend significantly on pH;[3,6] hence, to evolve hydrogen in a sustainable manner, it is necessary first to synthesize a highly active catalyst for water oxidation that is capable of lowering the activation energy of the anode reaction close to the thermodynamic minimum.[3] Significant attention has been devoted to the

DOI: 10.1021/cs5015157
ACS Catal. 2015, 5, 1499−1512

development of novel water-oxidizing catalysts that can be used in electrolyzers or as a part of photoelectrochemical devices.[4−6] Rare and expensive metals, such as platinum and iridium, are widely used for water oxidation in modern technology.[7] In contrast, cyanobacteria, algae, and higher plants, by controlling molecular environments and suppressing unfavorable oxidation reactions, manage to use abundant, nontoxic transition metals for the same purpose (Figure 2).[8−26]

Recently, there has been significant progress in improving the activity of water oxidation catalysts. Indeed, in some cases, the rate of oxygen evolution sustained by the water-oxidizing complex (WOC) or oxygen-evolving complex in PSII has been surpassed by artificial systems.[27−29] Nevertheless, research on the long-term mechanical and chemical stability of these catalysts is also necessary for commercial application. In the latter case, it is important that the system possess an ability to repair damage incurred during normal operation. When this is achieved in a spontaneous and autonomous fashion, the lifetime of the catalytic system can be significantly extended. This process, referred to as "self-healing", is highly significant for energy science because catalyst stability is a vital issue in both industrial and biological systems. Catalysts for multielectron reactions (such as water oxidation) are prone to structural rearrangement and instability during turnover; therefore, in this case, self-healing is especially important toward the retention of catalytic activity over an extended period of time.[30]

As discussed by Nosonovsky, degradation (deformation, fracture, chemical decomposition, etc.) and energy dissipation during friction and wear can be quantified in terms of entropy production.[31] These dissipative processes are irreversible and result in a net increase in entropy. Therefore, it seems contradictory that reorganization and self-healing, leading to a reduction in entropy, should occur. In nonequilibrium processes (such as friction), however, self-organization can be thermodynamically necessary. When the system operates far from equilibrium, the formation of organized secondary structures can result in reduced rates of entropy production. This way, self-organization and self-healing allow the system to shift back to equilibrium by moderating frictional forces. Similarly, when the system operates in a metastable state, self-organization can provide a thermodynamic force that drives the system to its stable equilibrium state (Figure 3). To induce self-healing, the system can be externally promoted to a metastable state by utilizing an energy input, such as heating, light or the application of an electrochemical potential.

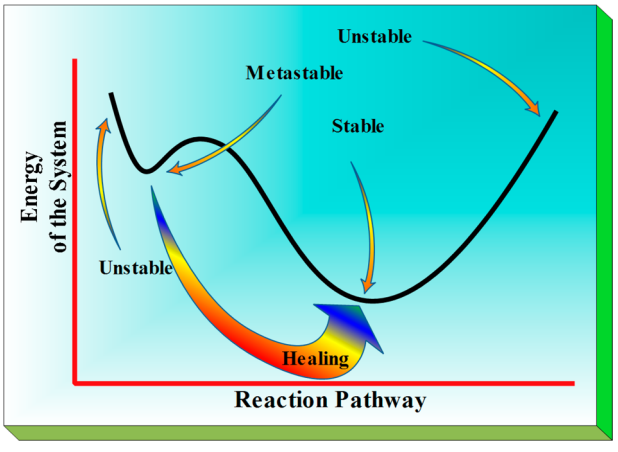

Figure 3. Possible reaction pathways (marked by arrows) related to the energy state of the system. Stable, metastable, and unstable points are indicated.

In material science, self-healing is defined as self-recovery of the initial properties of a compound following damage caused by the external environment or internal stresses.[32,33] Self-repair, autonomic healing, and autonomic repair are expressions commonly used to define such a property in materials.[34] However, self-healing is different from self-assembly and self-replication. Self-assembly[35] occurs when a disordered system of pre-existing components forms an organized structure without external direction.[32,35] Self-replication is any behavior of a system that yields construction of an identical copy of itself.[32]

As discussed above, self-healing can be an interesting strategy to increase robustness and extend the life of a compound, especially in cases where the repair or replacement of the compound is economically detrimental, dangerous, or impossible.

Self-healing systems have been classified into several groups. The first group includes those that are capable of autonomous self-healing and do not require any external intervention to restore the damage, such as certain biological systems.[36−39] In these biological systems, damage, such as a wound, is repaired by an autonomous self-healing process. The systems that require an external trigger to start the repair process are known as nonautonomous self-healing systems.[33,34] One example of a nonautonomous self-healing system could be a polymer matrix, in which heat can trigger a repair mechanism (such as filling of a crack) by an incorporated healing agent.

Different strategies have been employed toward the synthesis of self-healing compounds.[33,34] One strategy that has been implemented for polymer systems[40] involves the use of epoxy compounds as healing agents. The epoxy resin is stored within brittle macrocapsules embedded into the polymer. When damage occurs, the capsules fracture, and the healing agent is released, which then propagates into the crack with the help of capillary forces. In the next step, the healing agent reacts with a catalyst in the matrix, which starts the cross-linking reaction and hardening of the epoxy that seals the crack.[41,42] Other strategies used to propagate self-repair of polymer systems involve the incorporation of the healing agent into a material that requires heat to initiate healing.[43,44]

For metallic systems, three main self-healing methods have been developed. The first approach includes the formation of precipitates at the defect sites that immobilize further growth until failure.[32] The second method uses an alloy matrix with microfibers or wires that have the ability to recover their original shape after a deformation has occurred. This process usually requires heating above the phase transformation temperature. In a third approach, the healing agent, such as an alloy with a low melting temperature, is embedded into a metallic solder matrix.[32]

Nanomaterials are prone to both fast degradation and structural damage during use, and thus, self-healing strategies can be vitally important for the practical implementation of these materials.[32]

Triggered by injury, Nature has employed many different self-healing mechanisms ranging from single molecules to entire organisms and, thus, provides a source of inspiration for a variety of self-healing concepts that can be utilized in the design of catalyst materials.[39] As shown in detail in Figure 4, upon an injury, the biological response consists of three main steps: inflammatory response (immediate), cell proliferation (secondary), and matrix remodeling (long-term). Simple methods in synthetic self-healing materials mimic this three-step process: triggering (actuation),

DOI: 10.1021/cs5015157
ACS Catal. 2015, 5, 1499−1512

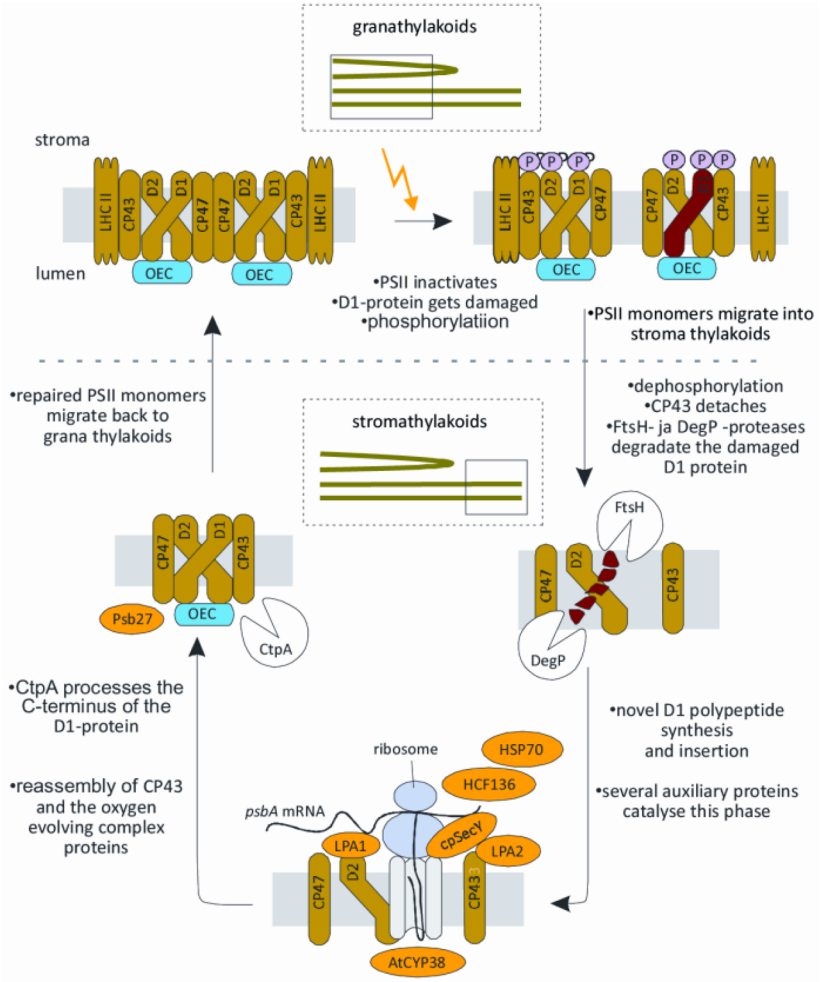

Figure 4. Photoinhibition−repair cycle of PSII in plant chloroplasts can be divided into five different phases. PSII supercomplexes, located in appressed thylakoids in the grana, are prone to photoinhibion. Under intense light, the PSII core proteins are phosphorylated. The D1 protein in damaged PSII is replaced by the new copy. PSII core protein phosphorylation facilitates the "migration" of the damaged PSII monomer to stroma-exposed thylakoid regions for repair. After core protein dephosphorylation, the D1 protein is degraded by the FtsH and DEG proteases. De novo synthesis of the D1 proteins occurs directly to the pre-existing parts of the PSII monomer and is assisted by a number of different auxiliary proteins (examples on yellow background). C-terminal processing of the pre-D1 protein and assembly of WOC occur before the PSII supercomplexes are reassembled in the appressed grana membranes.

transport of materials to the damaged sites, and chemical repair process.[45]

In the sections to follow, we first discuss some of the intricate processes that have evolved over millions of years to sustain water oxidation in living organisms and will explore how these mechanisms have inspired the development of Mn, Co, and Ni oxide-based water oxidizing catalysts with self-repair abilities.

PSII-WOC: NATURE'S WATER-OXIDIZING COMPLEX

The key role of manganese in oxygenic photosynthesis was first demonstrated in 1937.[46] Numerous methods have subsequently been applied to give insight into the structure of the water-oxidizing complex (WOC) in PSII. These have included electron paramagnetic resonance (EPR), electron nuclear double-resonance spectroscopy,[47−58] Fourier-transform infrared spectroscopy,[59−62] X-ray absorption spectroscopy (XAS),[8−11,63,64] X-ray diffraction on PSII crystals (protein crystallography), and other methods.[12−15,17−20,65] As a result of these studies, a consensus has emerged that the WOC contained four Mn, one Ca, and possibly one chloride ion.[66,67] The first key model suggested for the WOC was the "dimer of dimers" in which the Mn complex was assumed to be composed of two Mn "dimers" each comprising a di-μ-oxo-bridged Mn_2 unit.[8] Subsequently, Britt and co-workers proposed an alternative "dangler model".[54] In 2001, the first crystallographic model, with four Mn ions bound to PSII proteins, was presented at 3.8 Å resolution,[12] and in 2003, more protein ligands were identified.[13] In 2004, the research groups of Barber and Iwata provided, for the first time, information on the presence of Ca: the WOC was found to contain a Mn_3Ca in a cubic structural arrangement with the fourth Mn ion attached separately.[14] They proposed that three Mn and one Ca ion formed an elongated $CaMn_3(\mu\text{-}O)_4$ cubane-like structure together with four bridging oxygen atoms. In this model, the fourth Mn ion was connected to the cube by binding to one of the bridging oxygen atoms and was thereby positioned as a "dangler". In 2005, Biesiadka and co-workers presented an improved structure at 3.0 Å resolution.[15] In this study, a pyramid structure was proposed, involving three Mn atoms and the Ca atom, asymmetrically connected to Mn4. The bond lengths within the pyramid were determined as unequal, confirming a slightly distorted structure. Protein ligands were assigned with more confidence than was possible from the previous reports.

DOI: 10.1021/cs5015157
ACS Catal. 2015, 5, 1499−1512

Polarized extended X-ray absorption fine structure (EXAFS) data collected on protein crystals led to the proposal of four similar models for the $Mn_4(\mu\text{-}O)_n$ WOC core.[16]

In addition, using the crystallographic model of Barber and Iwata,[14] Batista, Brudvig, and Sproviero developed structural models of the WOC in different states by applying density functional theory (DFT) calculations.[68] Other studies investigated the location of chloride in the WOC.[69−71] These results showed, somewhat unexpectedly, that the chloride cofactor was not bound to any of the four Mn atoms or to the Ca ion. A further breakthrough occurred in 2011 when the resolution of PSII crystals was improved to 1.9 Å, enabling analysis of the WOC structure in atomic detail.[21] This key development has provided much more detail on the structure of the WOC, revealing the number and location of the bridging oxygen atoms, the location of putative water substrate molecules, and the precise arrangement of the amino acid side chains.[21] The structure proposed by Umena et al. consists of four Mn ions, one Ca ion, and five oxygen atoms that serve as oxo bridges linking the five metal ions.[21] In addition, four terminal water ligands were found, two of which were coordinated to the Ca ion and two to the "dangling" Mn ion (Mn(4)). Thus, the Mn−Ca cluster could be described as a $Mn_4CaO_5(H_2O)_4$ cubane-like structure (Figure 2). Eight of these ten atoms (five metals and five oxygen atoms) form a distorted cubic structure, with the Ca and three Mn ions occupying four corners and oxygen atoms forming the other four corners. The fourth Mn ion is located outside the cubane geometry and is linked by a di-μ-oxo bridge to two Mn ions within the cubane through one oxygen atom inside and the fifth oxygen atom outside the cubane structure.[65] Calculations of the Ca−O and Mn−O bond lengths revealed that the cubane-like structure is not symmetric. In addition, carboxylate and imidazole groups from several amino acids are coordinated to the $Mn_4CaO_5(H_2O)_4$ cluster.[21] In 2013, Shen and co-workers reported a Sr-exchanged cluster of $Mn_4CaO_5(H_2O)_4$,[65] that also catalyzes water oxidation; however, at reduced rates.

SELF-HEALING IN PSII

The photosynthetic apparatus in plants is prone to photoinhibition under natural light conditions. This is due to the oxidative chemistry of PSII and leads to deleterious reactions that disrupt the structure and function of the photosystem. It is intriguing that of the nearly 30 proteins in PSII, only the reaction center D1 protein (and the reaction center D2 to a much lesser extent) is vulnerable to damage and needs to be continuously replaced by a newly synthesized copy to keep the PSII complex functional.[72] It still remains unclear how photoinhibition of PSII damages the D1 protein and makes it susceptible to proteolytic degradation. However, it is important to note that the PSII repair cycle is one of the fundamental functions of the thylakoid membrane to maintain fluent photosynthesis. In the absence of such a repair cycle, the entire photosynthetic apparatus would be irreversibly deactivated on bright summer days.

Most PSII centers are located in supercomplexes in the appressed grana of the thylakoid membrane, whereas the repair machinery of PSII, particularly the ribosomes involved in the synthesis of the new D1 protein, are attached to nonappressed thylakoid regions. This structural arrangement means that lateral migration of the PSII complexes along the thylakoid membrane is an intrinsic feature of the PSII repair cycle in plant chloroplasts. However, it has become clear that under intensive light conditions, the area of appressed grana membranes decreases. This suggests that such "migration" of the complexes could be mainly due to the partial opening of the grana structures with the concomitant increase in the stroma-exposed thylakoid membranes.[73] Migration of PSII complexes or the opening of the appressed grana is regulated, at least partially, by reversible PSII core protein phosphorylation. At high light intensities, the PSII core proteins are phosphorylated in the supercomplexes within the grana, and the core protein phosphorylation facilitates the migration of the damaged PSII to the stroma-exposed lamellae for repair. Since the D1/D2 heterodimer is located in the heart of the PSII complex and ligates virtually all the cofactors essential for water splitting, it is evident that the repair cycle of PSII is an intricate process and involves a number of auxiliary and assisting proteins. Figure 4 depicts the major features of the PSII repair cycle and components involved in the process in plant chloroplasts.[72]

As noted above, the most active PSII centers are located in supercomplexes within appressed grana membranes, and this is where PSII photoinhibition and damage chiefly occurs. The PSII supercomplex, at the highest level of organization, consists of two PSII monomers with attached minor Chl *a*/*b*-binding antenna proteins (CP24, CP26, and CP29) and is surrounded by the trimers of the major light-harvesting Chl *a*/*b*-binding proteins known as LHCII. Under bright light conditions, the core proteins D1, D2, and CP43 are generally phosphorylated. When PSII becomes photoinhibited, concurrent damage of the D1 protein induces a still uncharacterized conformational change in the PSII supercomplex that results in (at least partial) detachment of the LHCII antenna and monomerization of the PSII dimer. Damaged PSII monomers then migrate to the stroma-exposed thylakoid regions for repair. Indeed, when damage has occurred in PSII, the functionality can be regained only via the repair cycle, which involves the replacement of the damaged D1 protein with a new copy by de novo synthesis.

In stroma-exposed thylakoid membranes (Figure 4), the damaged PSII monomer is dephosphorylated, particularly the D1 protein, and only thereafter does the damaged D1 protein become prone to proteolytic degradation. Before D1 degradation, the internal CP43 antenna protein detaches from the PSII complex, probably making space for the repair machinery to work on PSII. Extensive literature can be found describing the proteases involved in D1 protein degradation.[74] De novo synthesis and insertion of the new D1 protein into the pre-existing parts of the PSII complex are the next steps in the repair cycle. The D2 protein is apparently a docking site for newly synthesized D1 protein, which inserts into the membrane and interacts with the D2 protein.

The assembly of the $CaMn_4O_5(H_2O)_4$ cluster is followed by the assembly of the WOC proteins. PsbO is attached to the PSII complex first, followed by the assembly of the PsbP and PsbQ proteins. It is intriguing to note that the exact site of the WOC protein assembly has remained elusive. This process has been suggested to be either stroma-exposed, or to take place in the appressed thylakoid membranes. Nevertheless, after migration of the repaired PSII monomer to the appressed grana, the formation of the supercomplexes is tightly dependent on the presence of the WOC proteins in PSII.

PHOTOACTIVATION IN THE PSII-WOC

Another important issue in PSII that is related to self-healing is photoactivation. Photoactivation is the photoassembly of Mn, Ca, chloride, and water to the cofactor-depleted PSII in the presence of light, resulting in the formation of the Mn−Ca cluster (Figure 5).[75,76]

DOI: 10.1021/cs5015157
ACS Catal. 2015, 5, 1499−1512

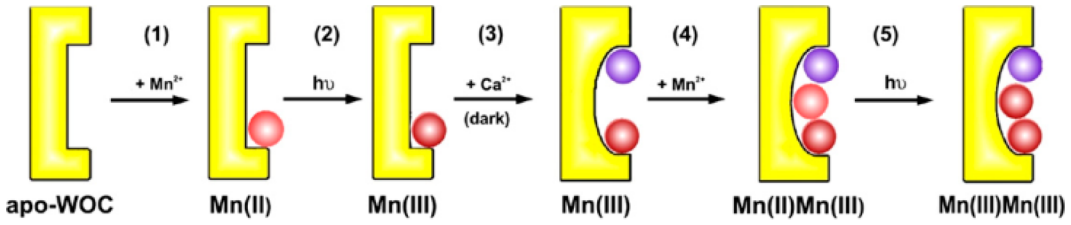

Figure 5. Methodology for removal of Mn_4Ca cluster by high pH treatment, for example, isolation of the cofactor-depleted PSII particles from isolated spinach PSII membranes, and reconstitution by photoactivation (assembly of the WOC is according to the two-quantum model).[81] The scheme depicts the stepwise binding of Mn(II) (light red) and Ca(II) (blue) to the cofactor-depleted PSII (yellow) as well as the photooxidation of Mn(II) to Mn(III) (dark red). Initially, a single Mn(II) is bound to the cofactor-depleted PSII and is oxidized by a first quantum of light. After binding of Ca(II) and a subsequent light-independent structural rearrangement (3), a second Mn(II) is bound (4) and photooxidized (5). The binding of the missing two Mn ions and chloride is not depicted in this scheme because it could not be kinetically resolved.[81] The model suggested by Cheniae and Martin,[82] which was basically confirmed in subsequent experiments using paired flash illumination.[83−86] Image and caption is from ref 81. Adapted with permission from ref 81. Copyright (2011) by Elsevier.

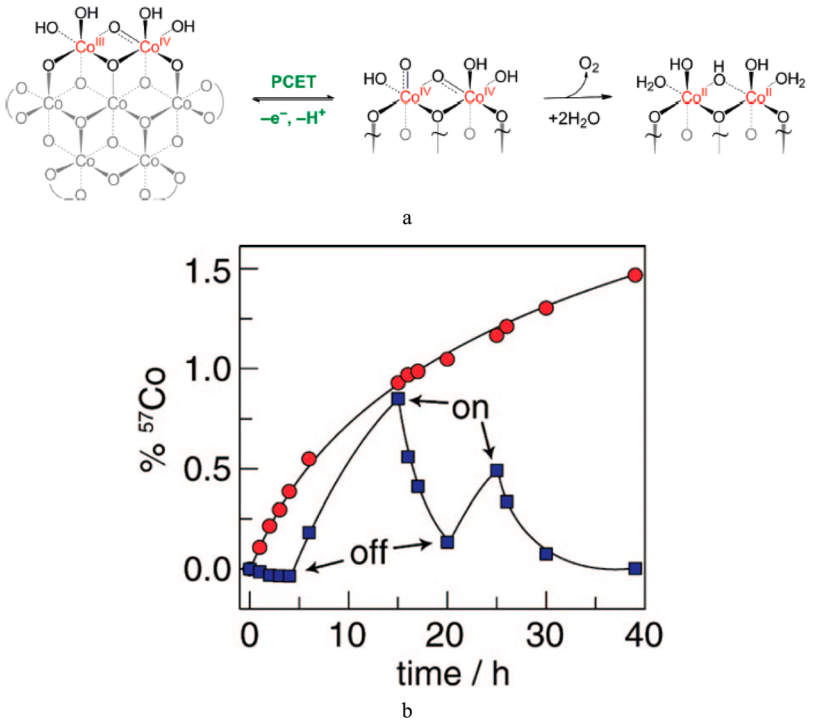

Figure 6. Proposed catalytic mechanism of the CoCF catalyst. PCET equilibrium step: [Co(III)−OH] ↔ [Co(IV)−O] + H^+ + e^-. Rate-limiting step: O−O bond formation (a). Image reprinted with permission from ref 99. Copyright (2010) by American Chemical Society. Percentage of ^{57}Co leached from films of the Co-Pi catalyst on an electrode with a potential bias of 1.3 V (NHE) (blue squares) turned on and off at the times designated and held at open circuit potential (red circles). At open circuit potential, high amounts of Co ions were released from the catalyst. After only 39 h, ∼1.5% of the cobalt ions was observed in solution. However, under a potential bias after 14 h, only 0.002% Co was detected in solution. Image and caption b reprinted with permission from ref 30. Copyright (2009) by American Chemical Society.

It is still unknown how the $CaMn_4O_5(H_2O)_4$ cluster is correctly assembled in PSII within plant chloroplasts, but more knowledge has accumulated from studies with cyanobacteria. A specific protein has been demonstrated as a Mn(II)-binding protein that is required for efficient delivery of Mn(II) to PSII in vivo.[77] It is known that the process is dependent on pH and, in addition, on the concentrations of free Mn(II), Ca(II), and bicarbonate ions. Photoactivation involves a two-step sequence (Figure 5). Ligation of Mn(II) first occurs at specific sites within the cofactor-depleted PSII and is not absolutely dependent on added Ca(II).[75,76,78] Then, in the presence of light, Mn(II) is oxidized to Mn(III).[75] The first step is critical because Mn(II) cannot be attached to the cofactor-depleted PSII. After oxidation of the Mn(II) ion to Mn(III), however, it binds strongly to the cofactor-depleted photosystem. It has been suggested that the photooxidation of the next Mn(II) is catalyzed by the −OH groups from $[Mn(III)−OH]^{2+}$ units because OH^- can serve as a better ligand than water to template the binding of the next Mn(II).[79] As discussed and reviewed by Nowaczyk, Ca(II) is an essential part of the active WOC with an ambiguous effect. It competes with Mn(II) for the photoactive site.[80] Low Ca(II) concentrations cause destructive photoligation of Mn(II) due to unspecific binding to the PSII donor side.[80] Most probably, Ca(II) promotes the light-independent rearrangement before the second photooxidation.[80] Photoactivation and self-healing processes have been well described for the Mn−Ca cluster in PSII.[81−87] The decomposed clusters can be self-repaired by a photoactivation process. The self-healing mechanism of this inorganic cluster could inspire self-repair strategies in the design of artificial water-oxidizing catalysts.

DOI: 10.1021/cs5015157
ACS Catal. 2015, 5, 1499−1512

SELF-HEALING PROCESSES IN SYNTHETIC WATER-OXIDIZING CATALYSTS

The concept of utilizing self-healing strategies toward improving the stability of various materials was presented many years ago;[87,88] however, its application in water electrolysis is relatively new. Since the self-healing cobalt oxide water oxidation catalyst was reported by the Nocera group in 2009,[30] the concept has started to rapidly attract more attention, and several catalyst materials with self-healing ability are now known.[84,89−91] In the following sections, we will discuss a few selected milestones of the development of cobalt, nickel, and manganese oxide-based water oxidation catalysts and compare reports on self-healing mechanisms that lie behind the recently achieved prolonged catalyst lifetimes.

Cobalt Oxides. In 1968, Glikman and Shchegoleva observed that the introduction of powdered metal oxides, such as cobalt oxides (also Pt, Pd, and Mn oxides) into a solution of Ce(IV) perchlorate (a sacrificial oxidant) resulted in vigorous oxygen evolution.[92] In the 1990s, Jiang et al. prepared highly active mixed cobalt oxide/hydroxide catalysts by reactive electrodeposition from a $CoCl_2$ solution onto nickel mesh or titanium foil substrates in concentrated alkaline solutions.[93,94]

A self-healing mechanism in in-situ-deposited cobalt oxides was first mentioned by Kanan and Nocera in 2008.[6] A cobalt oxide catalyst film (CoCF) was electrodeposited from a solution containing cobalt and phosphate ions at neutral pH. XRD data suggested that the cobalt catalyst film was largely amorphous. Proposed mechanisms for the H_2O/O_2 redox cycles at the Co centers suggested the involvement of Co(II), Co(III), and most probably Co(IV) oxidation states during water oxidation.[95] The water oxidation current was found to rapidly diminish when no Co(II) ions were present in the electrolyte. The fate of the Co and phosphate ions during electrodeposition and catalyst operation was examined when the oxide film (Co-Pi) was prepared from a radiolabeled solution containing ^{57}Co and ^{32}P isotopes.[30] Held at open circuit potential, the film was observed to gradually dissolve. On the other hand, when a potential bias of 1.3 V vs NHE was applied (also sufficient for water oxidation to occur), no film dissolution was observed until the potential bias was removed. This process could be reversed when a buffering electrolyte (in this case a phosphate buffer) was present. It has been described as self-healing of the catalyst film, which entails the redeposition of the leached Co(II) ions at operational potentials as an amorphous phosphate-rich Co(III) oxide catalyst film, such "healing" the degrading catalyst film simultaneously with O_2 evolution. In the absence of a buffering electrolyte, the film degradation was irreversible: the protons generated in the vicinity of the catalyst surface, when not transported into the bulk of the electrolyte by proton acceptors, accumulate and cause a local decrease in pH, leading to the dissolution of the catalyst film. As a consequence, the presence of a buffering electrolyte (such as a phosphate buffer) was confirmed as essential for prolonged catalyst operation (Figure 6).

Further studies by Nocera and co-workers on the CoCF confirmed that the presence of a proton-accepting buffer solution was essential to prolonged catalytic function. It was also shown that exchange between various proton-accepting buffers was permitted: the catalyst film was also found operational in borate instead of phosphate buffers or even natural seawater (with the addition of a buffer).[96] This phenomenon was linked to the relative instability of Co(II) compared with Co(III) during catalyst turnover.[30,97]

The CoCF was also examined by Dau and co-workers, who employed X-ray absorption spectroscopy to elucidate the structure and oxidation state of the cobalt centers in the catalyst film.[98a] This study proposed that the active catalytic center of the CoCF is composed of interconnected complete or partial Co(III) cubane clusters bearing a strong structural resemblance to the WOC in PSII. The possible ligation with K^+ ions present in the buffer solution was suggested to lead to the formation of $Co_3K(\mu\text{-}O)_4$ cubanes, analogous to the $Mn_3Ca(\mu\text{-}O)_4$ cubane motif of the natural water-oxidizing complex. Pair distribution function analysis by the Tiede group indicated that the catalyst is essentially a cobalt dioxide lattice sheet containing a Co_4O_4 cubane-type structure, composed of 13−14 cobalt ions.[98b] In the catalyst structure, phosphate is present as a disordered component.[98b]

The mechanism of the CoCF-catalyzed oxygen evolution reaction was further investigated by Surendranath et al., focusing on the role of the proton-conducting buffer in the catalytic process.[99] Electrokinetic studies, mainly Tafel analysis, were carried out in neutral phosphate buffer solutions. In the absence of the buffer, the Tafel slope increased 3-fold, indicating a dramatic drop in the rate of oxygen evolution. A relatively low concentration of phosphate (0.03 M) was sufficient to maintain a Tafel slope of 59 mV/decade; a further increase in buffer concentration did not affect the rate of the oxygen evolution reaction. A first-order dependence of the current density on pH (inverse first-order dependence on the activity of protons) was also established. On the basis of these observations, as well as ^{18}O-labeled experiments and theoretical considerations, the authors proposed a reversible equilibrium step involving one proton and one electron ($A \leftrightarrow B + e^- + H^+$), followed by a rate-limiting $B \rightarrow C$ step. The equilibrium step involves proton-coupled electron transfer (PCET) between Co(III)−OH and Co(IV)−O species, with phosphate as the proton acceptor. This equilibrium was also termed "catalyst resting state". An O−O bond is formed in the irreversible chemical-rate-limiting step, and the resulting oxygen molecule is released. The edge-sharing octahedral structure was proposed for the CoCF catalyst by Nocera and co-workers.[100] Gerken et al.[101] and Surendranath et al.[97] further investigated the structure and catalytic mechanism of the CoCF through Pourbaix analysis, EPR, and XAS studies, leading to similar conclusions. In agreement with the octahedral model, the study found that the catalyst mainly consisted of stacked oligocobaltate lamellae, forming a three-dimensional layered double-hydroxide structure. These investigations into the structure, formation, and catalytic mechanism of the CoCF provide deeper insights into the observed self-healing behavior. Under buffered, neutral to alkaline conditions, aqueous Co^{2+} ions in the solution are oxidized upon the application of a sufficiently positive potential and deposited as a Co(O)OH species. This material is further oxidized to the above-mentioned catalyst resting state, a mixed Co(III)−OH and Co(IV)−O oxide. In alkaline solutions, the catalyst in the resting state is oxidized to Co(IV) oxide, which reacts with the H_2O substrate, resulting in the release of oxygen gas and the reduction of the catalyst to Co(III) (oxy)hydroxide. This completes the cycle, the aqueous Co^{2+} species leached from the dissolved, corroded film redeposit (with the appropriate bias applied) via the same mechanism as the original film formation. Gerken et al.[101] point out that the described mechanism, including the self-healing process, is a direct consequence of the thermodynamics of the system.

Drawing inspiration from the success of the CoCF, many other cobalt oxide catalysts have been synthesized with the aim of

DOI: 10.1021/cs5015157
ACS Catal. 2015, 5, 1499−1512

improving their performance even further. Jiao et al. published a series of studies on a silica-templated, nanostructured, mesoporous Co_3O_4 spinel oxygen-evolving catalyst.[102] These spinel structures are of special interest because they comprise Co(II) tetrahedra and Co(III) octahedra, Co_4O_4, which bears high structural resemblance to the PSII-WOC. Grewe et al. tested a very similar silica-templated mesoporous Co_3O_4 spinel in electrochemical water oxidation in a pH 13 KOH electrolyte.[103] Incorporation of small amounts of iron into the mesoporous structure was shown to result in decreased symmetry (a more disordered structure) with greater film porosity and higher activity. Instead of using Co(II) as a cobalt source during electrodeposition of the cobalt oxide film, Han and co-workers deposited CoO_x catalyst films from cobaloximes.[104] Cobaloximes are generally used as water reduction catalysts,[105] but when electrodeposited from buffered mildly alkaline electrolytes at highly positive potentials (+1.7 V vs SHE), the formation of a water-oxidizing cobalt oxide film was observed. The activity was found to depend on the cobaloxime precursor. The maximum current density measured using the best-performing film was 2.6 mA cm^{-2} when biased at 1.3 V vs SHE at pH 9.2 (η = 610 mV). This activity is comparable to the 1 mA cm^{-2} current obtained from the CoCF at η = 470 mV. The authors stressed the stability of the film morphology when the catalysts were operated on a longer term, which was confirmed to be close to 100% over 8 h of continuous operation in a borate buffer. The good stability observed at mildly alkaline pH (pH 9.2) in the presence of a proton-accepting electrolyte agrees well with the findings of Nocera and co-workers[101] on the CoCF catalyst. Indeed, the authors considered the possibility of a dynamic self-repair mechanism occurring during oxygen evolution.

Nickel Oxides. Nickel oxide has been used in energy storage applications since the late 19th century.[106] Nickel electrodes were typically fabricated by cathodic electrodeposition and used as cathode materials in batteries.[107] In the 20th century, Raney-nickel became the main catalyst material of choice in commercial alkaline water electrolyzers.[108] In terms of water oxidation catalyst design, nickel oxide/hydroxides[109,110] and mixed nickel oxides, mostly perovskites (for example, $LaNiO_3$)[111] and spinels such as $NiCo_2O_4$[112] and a variety of Ni-based catalysts, have been tested with a view to improving catalytic activity and minimizing the oxygen evolution overpotential. Appleby et al.[109] and Hall[110] building on mechanistic studies by Lu et al.,[113] which suggested that nickel oxyhydroxides were the active surface species in nickel oxide catalyzed water oxidation, reported $Ni(OH)_2$-impregnated porous nickel electrodes. Nickel oxyhydroxide was found to form when $Ni(OH)_2$ was electrochemically oxidized. The surface morphology of the best-performing nickel hydroxide impregnated porous nickel electrode could be described as submicrometer-sized spherical nodules and has some similarity to that of the active cobalt oxide electrodes discussed earlier.

While studying nickel oxide batteries, Corrigan and co-workers noticed that Fe impurities in the electrode material (possibly introduced from rust staining) led to the formation of O_2 bubbles, which, while detrimental to the battery charge process, presented a new approach to alkaline water electrolysis.[114] As little as 0.01% iron, coprecipitated with nickel oxide, led to a reduction in the oxygen evolution overpotential, and higher concentrations of iron in iron/nickel oxyhydroxide composite materials was found to efficiently catalyze water oxidation. At 10% iron content, the overpotential was reduced by 200 mV to 250 mV (at 80 mA/cm^2 current density), as compared with pure nickel oxide. The Tafel slope decreased from 70 to 25 mV/decade in a 25% KOH electrolyte. Corrigan's work[114] opened up a field of research into composite nickel oxide water-oxidizing anodes. Merrill and Dougherty confirmed Corrigan's findings by comparing the catalytic performances of a range of transition metal composites. They concluded that a catalyst film deposited from a solution containing equal concentrations of $NiCl_2$ and $FeCl_2$ onto Pt foil had the highest activity when measured in a 1 M KOH solution.[107] Pletcher and co-workers also investigated electrodeposited composite hydroxides of nickel with Fe, Co, Cr, Mn, and Cu.[115] The addition of manganese and copper was found to be detrimental to performance when compared with $Ni(OH)_2$. Copper and chromium addition improved performance slightly, but once again, the highest activity was observed when 10% iron was present in the $Fe/Ni(OH)_2$ composite.

The Nocera group, based on their earlier results using the CoCF, demonstrated that similar approaches could be utilized to obtain active nickel oxide oxygen-evolving catalysts.[116] The "Ni–B_i" film, deposited from dilute solutions of Ni^{2+} in the presence of borate ions at pH 9.2 and operated at the same pH could present a more benign alternative to nickel oxide catalysts designed to function in highly alkaline electrolytes. Although more environmentally friendly, the Ni–B_i film cannot produce the high oxidation current observed previously in alkaline electrolyzers. At 1.3 V constant applied potential vs SHE, the current recorded was 1.3 mA/cm^2, and the Tafel slope was 58 mV/decade. It has been argued, however, that operation at lower current density can be more energy-efficient because less vigorous bubble formation results in smaller Ohmic losses through the cell.[116]

Electrodeposition from nickel complexes, rather than simple nickel salts, has the potential to gain better control over film morphology. Spiccia and co-workers demonstrated the influence of the molecular precursor on activity and long-term stability of nickel oxide water oxidation catalysts.[117,118] Two molecular complexes, $[Ni(NH_3)_6]Cl_2$ and $[Ni(en)_3]Cl_2$ (en = 1,2-diaminoethane) were used as precursors to deposit nickel oxide at pH 9.2. The best-performing NiO_x-en films generated 1.8 mA/cm^2 anodic current at 1.1 V vs Ag/AgCl, representing an improvement in terms of current per electrode area over the Ni–B_i film. The Tafel-slopes, however, were measured as 104–105 mV/decade for all films deposited from the different precursors, which was higher than that of the Ni–B_i films. Because Tafel slopes are intensive measures of intrinsic activity independent of surface area, these results suggest that the main advantage of the complex-precursor materials lies in their higher electrochemically active surface area (the NiO_x-en films have a nanoporous surface structure with dendritic surface features, with a well-defined particle size between 300 and 350 nm).

Self-repair of nickel oxide-based water oxidation catalysts has not had significant literature coverage so far, mainly because of the outstanding stability of these materials under typical operating conditions. The Pourbaix diagram of nickel[119] clearly shows that below pH 9, Ni^{2+} is the dominant stable form of Ni in an aqueous solution over a wide potential range. Below pH 9, therefore, nickel oxide-based water oxidation catalysts would irreversibly dissolve (until an equilibrium between the dissolved and solid phases is reached; this is dependent on the anions present in the electrolyte solution). In this case, even the application of a large positive bias would still not be sufficient to induce redeposition-self-healing of a nickel oxide or hydroxide phase. In traditional alkaline electrolysis and under more recently adapted, less harsh basic conditions (e.g., borate buffers, as discussed above), however, the situation is very different. Recent mechanistic studies by Nocera and co-workers suggest that, at alkaline pH, the nickel oxide-based

DOI: 10.1021/cs5015157
ACS Catal. 2015, 5, 1499–1512

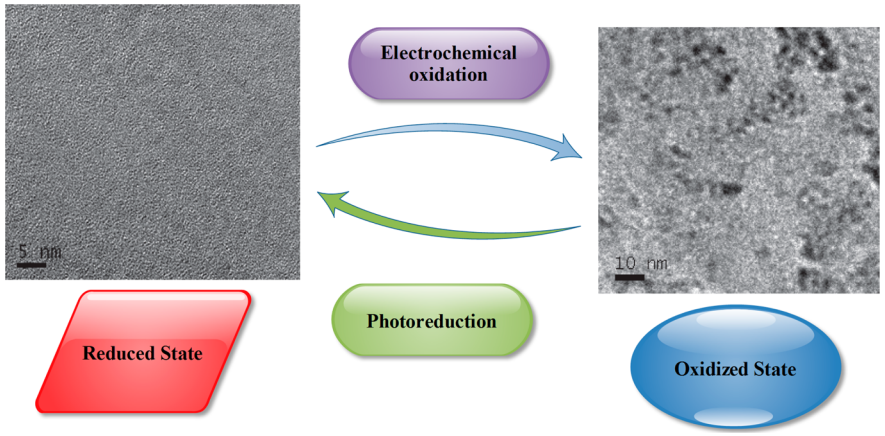

Figure 7. Self-healing cycle for Mn oxide proposed by Spiccia and co-workers. High-resolution transmission electron microscopy images. Right: Nafion film showing presence of manganese oxide nanoparticles formed on electrooxidation of $[Mn_4O_4L_6]^+$ at 1.0 V (versus Ag/AgCl). Left, Nafion film examined after introduction of $[Mn_4O_4L_6]^+$ into the film. Images and caption are reprinted with permission from ref 135. Copyright Nature Publishing Group (2011).

catalyst cycles between NiO(OH) and mixed Ni(II)/Ni(III) hydroxide phases during operation, all of which phases are highly insoluble in water.[90] Continuous operation, in contrast with Co- or Mn-based water oxidation catalysts, was found to initially improve, rather than decrease current drawn from the device. This process is also referred to as anodization. Excellent long-term stability has been demonstrated for numerous Ni-based catalysts used in water oxidation.[116,117,120]

While representing one of the longest-studied group of electrode materials (both as battery cathodes and water oxidizing anodes) that are remarkably active and stable, especially in concentrated bases, it needs to be noted that nickel oxides are also more toxic and less Earth-abundant than other transition metal oxides, such as manganese oxides.

Manganese oxides. Following the initial studies by Glikman, Shcheglova[91] and Morita[121,122] on water oxidation using metal oxides (including Mn-oxides), Shafirovitch and Shilov first suggested that Mn-oxo-based catalysts could bear functional similarity to the PS-II WOC.[123,124] The turnover rate of the PSII-WOC is 100−400 s^{-1} in living microorganisms (such as algae), and up to 1000 turnovers per second were measured in vitro.[125] This catalytic turnover rate is considered a benchmark for synthetic mimics. Inorganic analogues of the WOC face many challenges: apart from trying to achieve high activity, coupling the water oxidizing catalyst to light-harvesting antennae and ensuring its long-term stability are some of the main issues that need to be addressed. As discussed above, in the natural system, these functions are carried out by the surrounding protein matrix. Synthetic systems need to provide functional analogues to these extremely complex biological structures.

Najafpour and Kurz, aiming at simulating the $CaMn_4O_5(H_2O)_4$ cluster in PSII, showed that the incorporation of Ca ions into Mn oxides can improve the catalytic activity of these synthetic Mn oxides.[126] Wiechen et al. pointed out that birnessites possess an intriguing similarity to the PSII-WOC if the μ-oxo-bridged Mn_4O_5Ca core of the WOC cluster is considered as part of a possible extended oxide structure.[127] Kurz and co-workers prepared a series of birnessite clays with intercalated alkali and alkali earth ions.[127] The activity, based on oxygen evolution measurements from a pH 2 Ce(IV) oxidant solution, was in the order of Ca(II) > Sr(II) > Mg(II) > K(I). Similar experiments, in which the natural WOC was depleted of Ca(II) and replaced with other ions, resulted in the same order of activity. This finding further strengthened the concept that Ca birnessites can be considered not only structural, but also functional mimics of the PSII-WOC.

Suib and co-workers compared the activity of synthetic layered K^+-birnessites to tunnel-structured manganese oxides and to amorphous manganese oxides (AMO).[128] On the basis of oxygen evolution experiments, in a system similar to that used by Kurz and co-workers,[126,127] AMO was found the most active. The AMO was found to contain randomly oriented sheets of a hexagonal H^+ birnessite-like structure (resembling MnO_2 with a large number of cation vacancies). Najafpour and co-workers also showed that different Mn oxide phases, in the presence of Ce(IV) or in an electrochemical water oxidation process, transform to a layered Mn oxide phase after a few hours.[129,130]

The intriguing fact that both molecular Mn oxo complexes[126,131,132] and heterogeneous manganese oxides can represent structural and functional analogues to the PS-II WOC, led to further investigations of the transformations that these catalyst materials go through during operation.[133−135] Interestingly, these studies also led to new insights into the self-healing ability of some of these catalyst systems.

A first example of such molecular-heterogeneous transformations in the field of Mn-based water oxidation catalysts was reported by the Spiccia group during investigations of a tetranuclear Mn cluster (also referred to as a "cubane", $[Mn_4O_4L_6]^+$; L: diarylphosphinate). When embedded into a Nafion polymer matrix deposited on a conductive electrode and irradiated with visible light, this cluster was shown to function for up to 3 days with minor loss in activity.[125] A PSII mimic, combining the above-mentioned Mn-WOC catalyst with a light-harvesting layer similar to that employed in a dye-sensitized solar cell (DSC) was also developed. In this case, visible light was used as the only energy source to achieve water oxidation catalysis.[133,134]

In 2011, Hocking et al.[135] proposed a different mechanism for water oxidation by the $[Mn_4O_4L_6]^+$ compound. The cluster was shown to dissociate in Nafion, yielding Mn(II) species that were converted into a disordered Mn(III/IV) oxide phase upon electrooxidation. It was further demonstrated that in situ cycling between the Mn(II) photoreduced product and an oxidized, disordered Mn(III/IV) oxide phase most likely forms the basis of the observed water oxidation catalysis. That is, irradiation of the oxide with visible light results in the release of oxygen and

DOI: 10.1021/cs5015157
ACS Catal. 2015, 5, 1499−1512

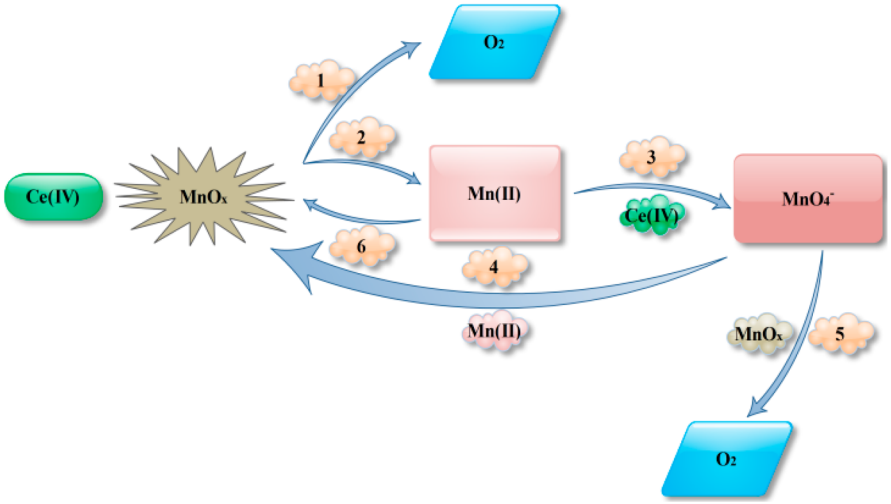

Figure 8. Self-healing in water oxidation by Mn oxides in the presence of Ce(IV). 1: Oxygen evolution was detected by an oxygen meter. The origin of oxygen is water. 2: Mn(II) was detected by EPR (see text). 3: MnO_4^- formation could be detected by UV−vis spectrophotometry in reacting Mn(II) and Ce(IV). 4: It is known that in the reaction of Mn(II) and MnO_4^- at different pH values, Mn oxide is produced. 5: MnO_4^- in the presence of Mn oxide oxidizes water. In the reaction, MnO_4^- reduces to Mn oxide. 6: Mn(II) in the presence of Ce(IV) forms Mn oxide. In a typical experiment, the reaction of $MnSO_4$ in the presence of Ce(IV) (1.0 M) forms MnO_2, which can be detected by XRD. Images and captions reprinted with permission from ref 89. Copyright (2013) by Royal Society of Chemistry.

photoreduction to Mn(II) species, which are converted back to the oxide by the constantly applied bias. The bias is necessary for the oxide catalyst to self-heal or regenerate so that further water oxidation catalysis is possible (Figure 7).

To demonstrate the cycling between the Mn oxidation states, K-edge XAS[135] was used to probe the fate of the cubane cluster when dissolved in acetonitrile and when embedded in a Nafion film coated on a glassy carbon electrode. A comparison of the spectrum of $[Mn_4O_4L_6]^+$ measured in acetonitrile with that measured immediately after loading of the cluster in Nafion revealed a shift of the X-ray absorption near-edge structure (XANES) peak to a lower energy immediately upon the loading of $[Mn_4O_4L_6]^+$ into Nafion, which was consistent with the reduction of the cluster to a Mn(II) compound.[135] The EXAFS and its Fourier transform were consistent with a Mn(II) inner sphere occupied by six oxygen donors with no ordered second sphere (that is, not part of a crystal lattice).[135] Electrooxidation of the Mn(II) product at a potential of 1.0 V (vs Ag/AgCl) shifted the XANES rising edge to a higher energy. The XANES peak intensity of the reoxidized product lay between that expected for Mn(III) and Mn(IV) and was consistent with a material having an average oxidation state of ∼3.8, similar to that of oxidized cubane. However, the XANES spectra of the electro-oxidized product and the $[Mn_4O_4L_6]^+$ cluster differed, and thus, it was concluded that $[Mn_4O_4L_6]^+$ may not be responsible for the prolonged water oxidation catalysis.

Further studies then showed very similar EXAFS patterns for the products of electrooxidation of Mn(II), $[Mn_4O_4L_6]^+$ and $[(bpy)_2Mn(O)_2Mn(bpy)_2]^{3+}$ in Nafion at 1.0 V (vs Ag/AgCl). This indicated that, upon electrooxidation in Nafion, all three Mn precursors generate a compound with a structure very similar to a layered Mn oxide type material.[135,136] In addition, NMR experiments were conducted to show that decomposition of $[Mn_4O_4L_6]^+$ occurs in Nafion. The ^1H and ^{31}P spectra of $[Mn_4O_4L_6]^+$ on Nafion films exhibited peaks corresponding to those of the protonated ligand, indicating partial or total dissociation of the ligands from the cluster.[135] Finally, high resolution TEM studies, undertaken on both the oxidized and reduced states of Nafion films doped with either $[Mn_4O_4L_6]^+$ or Mn(II) from an acidified solution, led to the identification of nanoparticles (10−20 nm in diameter) in the TEM image of the oxidized films obtained from both Mn(II) and $[Mn_4O_4L_6]^+$, whereas no nanoparticles were found for the reduced state. This is consistent with the XAS results, which indicated that in situ reduction of the Mn-precursors occurs upon doping into the Nafion membrane, wherein Mn(II) species with no higher order structure are formed.[137] EPR experiments provided further confirmation that the Mn precursor complexes are reduced to Mn(II) within the Nafion film and are subsequently oxidized to EPR silent manganese oxide materials. Detailed electron diffraction analysis established that the structure of this Mn oxide catalyst corresponds to that of layered birnessite.[138] This provides clear evidence of self-healing, similar to the observations of Nocera and co-workers on cobalt oxides.[97] However, it was also found that despite the fact that the same Mn oxide phase is formed from a variety of Mn precursors, the size, crystallinity, and catalytic activity can be enhanced through judicious choice of the precursor.[137] Furthermore, a very recent study, applying L-edge XAS and Resonant Inelastic X-ray Scattering (RIXS), has established differences in the electronic structure of the Mn oxide phase that very likely contribute to the higher catalytic activity of the water oxidation catalyst derived from some molecular precursors.[139]

Following the above-described studies in electrochemical systems, a new self-repair pathway for Mn oxide in the presence of chemical oxidants and in the presence of $(NH_4)_2Ce(NO_3)_6$ (Ce(IV)) was reported by the Najafpour group.[89] Under these conditions, in addition to oxygen, MnO_4^- is also formed. This is in agreement with the Latimer diagram of Mn; namely, that oxidation of Mn(II) or Mn(III) to MnO_4^- is more facile than the oxidation of MnO_2 to MnO_4^-.[89]

The standard reduction potential of Ce(IV) is 1.5 V vs NHE, which can hardly oxidize MnO_2 to MnO_4^-. Thus, it was proposed that Ce(IV) oxidizes the Mn(II) or Mn(III) species on the surface of the Mn oxide to MnO_4^-. It was also shown that the reaction of Mn(II) with Ce(IV) in solution produces MnO_4^-. The results of

DOI: 10.1021/cs5015157
ACS Catal. 2015, 5, 1499−1512

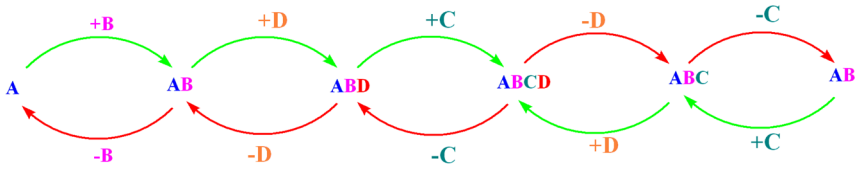

Figure 9. Decomposition and self-healing of the PSII-WOC (during photodeactivation) or metal oxides (during catalytic operation) could be summarized by this simple schematic image. In this image, each structure contains only a few components. The attachment or removal of these components results in self-healing (green arrow) or decomposition (red arrows).

these experiments suggested that MnO_4^- may be formed by the oxidation of Mn(II) (leached from the Mn oxide catalyst) by Ce(IV) present in the electrolyte.

More interestingly, at the end of the reaction and after consumption of Ce(IV), no MnO_4^- was observed. This shows that after catalyst decomposition to MnO_4^- (eq 4), there is a self-healing reaction that repairs the catalyst once again (eq 5):

$$5Ce(IV) + Mn(II) \text{ from catalyst} \rightarrow MnO_4^- + 5Ce(III) \quad (4)$$

$$MnO_4^- \rightarrow \text{Mn oxide} \quad (5)$$

A MnO_4^- solution in the presence of the Mn oxide catalyst showed a linear reduction in concentration, which suggests that a reaction takes place between MnO_4^- and the Mn oxide. This indicates that Mn oxide is necessary for the reduction of MnO_4^-.

The consumption of MnO_4^- in the presence of Mn oxides can be explained by at least two possible reactions: first, MnO_4^- can react with the Mn(II) ions resulting from catalyst decomposition and redeposition as Mn oxide (Figure 8, pathway 4); second, MnO_4^- acts as an oxidant, and Mn oxide, as a water-oxidizing catalyst, reacts to oxidize water (Figure 8, pathway 5). In this second case, MnO_4^- is reduced to MnO_x, which can also be considered a self-healing process. Indeed, in 1979, the Shilov group observed oxygen evolution when MnO_4^- was in contact with solid MnO_2.[124] The isotopic composition of oxygen showed that the reaction was indeed a water oxidation reaction. In both cases, the reprecipitated MnO_2 on the catalyst surface is amorphous,[130] and active toward water oxidation.

SELF-HEALING IN BIOLOGICAL VS SYNTHETIC WATER OXIDATION CATALYSTS

Among different compounds applied in water oxidation, metal oxides can be designed as self-healing compounds, but the repair mechanism is completely different from natural systems. In other words, whereas PSII uses a complex biological procedure to repair itself, metal oxides use different redox reactions to repair their structures, as we have shown through a few examples above. As discussed by Urban,[140] it is important to note that self-healing processes are performed by the replacement of "outdated" components in biological systems, which is difficult to mimic in synthetic systems. However, the systems introduced here, similarly to biological systems, use decomposed and "outdated" components (Co(II), Mn(II), or MnO_4^-) for self-healing. Such reactions for metal complexes are not easy to perform because, usually, decomposed or oxidized ligands cannot be fixed easily. On the other hand, self-healing related to processes during the biological water oxidation reaction, as well as many other biological processes, is much more complex than the self-healing behavior of Mn or Co compounds discussed here in the context of water oxidation. However, some similarities can be observed between the formation and decomposition processes within the Mn−Ca cluster in PSII and those of Mn- or Co-based inorganic water oxidizing catalysts. As shown in Figure 9, both the Mn−Ca cluster in PSII and Mn or Co oxides can be considered to be composed of a few simple "building blocks":

1. Mn−Ca cluster: Mn, Ca, and O
2. Mn oxides: primarily Mn and O
3. Co oxides: primarily Co and O
4. Ni oxides: primarily Ni and O

Decomposition (red arrows in Figure 9) or self-healing (green arrows in Figure 9) reactions can occur within these structures. The detachment and reattachment of these components is related to the decomposition and self-healing processes, respectively.

CONCLUSIONS

Water oxidation catalysis constitutes the bottleneck in the development of artificial water splitting utilizing sunlight as the energy source. The compounds that catalyze natural water oxidation or other multielectron reactions are prone to instability during rapid catalytic turnover. The high rates of damage and repair observed in the only natural system that is capable of sustaining water oxidation, PSII, make it an important model to study in the quest for a fundamental understanding of key aspects of self-healing. It is important to learn about and apply different aspects of self-healing from the natural system in the design of new water-oxidizing compounds with self-healing ability. Even though self-healing in material science and biology occurs according to completely different mechanisms, a number of key similarities exist between these two systems. These synergies offer promise for the design of novel water-splitting systems assembled from earth-abundant materials that possess the ability to provide cheap and sustained fuel production for future generations. Among different strategies for achieving self-healing reactions, the self-healing processes that are performed by the replacement of "outdated" components in biological systems are very important but difficult to mimic in synthetic systems. Metal oxide catalysts involved in the water-oxidizing reaction often use such decomposed components for self-healing. Under conditions prevalent during water oxidation, kinetically active (labile) ions are removed from the heterogeneous catalyst. On the other hand, high-valent metal ions, such as Mn(VII) MnO_4^- can be formed in the water-oxidation reaction, causing the decomposition of the catalyst material. Self-healing reactions can efficiently reintegrate such species into the catalyst.

In addition to being able to self-heal, the catalysts need to have a number of other highly desirable properties. They should (i) consist of abundant elements; (iii) be easily synthesized and manufactured, and at low cost; (ii) exhibit high stability under catalytic cycling; (iv) exhibit high catalytic activity and efficiency; and (v) be environmentally friendly. Of the potential candidates and in the absence of molecular catalysts that meet these criteria, manganese oxides are particularly attractive candidates for application as water-oxidizing catalysts in artificial photosynthetic systems because they fulfill most of these requirements. In

DOI: 10.1021/cs5015157
ACS Catal. 2015, 5, 1499−1512

addition to the optimization of electrolytic systems that can function under benign noncorrosive conditions, the integration of such self-healing catalysts with photoactive materials to create photoelectrochemical devices or heterogeneous systems capable of using only sunlight to generate fuels (from water or carbon dioxide) should be an area of intense focus from now into the foreseeable future. To maximize sunlight to fuel conversion efficiency, however, catalytic turnovers commensurate with the flux of solar radiation need to be achieved with the lowest possible energy input (i.e., as close as possible to reaction thermodynamics). Moreover, the materials need to satisfy the additional stringent requirements of long-term stability or self-healing under continuous illumination.

AUTHOR INFORMATION

Corresponding Authors

*Phone: (+98) 24 3315 3201; Fax: (+98) 24 3315 3232. E-mail: mmnajafpour@iasbs.ac.ir (MMN).
*Phone: (+7) 496 7731 837; Fax: (+7) 496 7330 532. E-mail: suleyman.allakhverdiev@gmail.com (SIA).
*Phone: (+61) 3 9905 4526; Fax: (+61) 3 9905 4597. E-mail: leone.spiccia@monash.edu (LS).

Notes

The authors declare no competing financial interest.
△M.M.N. and M.F. contributed equally to this paper.

ACKNOWLEDGMENTS

M.M.N. and D.J.S. are grateful to the Institute for Advanced Studies in Basic Sciences, and the National Elite Foundation for financial support. S.I.A. was supported by a grant from the Russian Science Foundation (No: 14-14-00039). E.M.A. was supported by the Academy of Finland (No. 118637). The Monash authors acknowledge financial support from the Monash Institute of Graduate Research and Faculty of Science in the form of scholarship support and a Postgraduate Publication Award (M.F.), and the Australian Research Council (through the ARC Centre of Excellence for Electromaterials Science, Grant No. CE140100012, L.S.). J.R.S. was supported by a grant-in-aid for Specially Promoted Research (No. 24000018) from JSPS, MEXT, Japan. The authors are grateful to Mika Keränen for his assistance with Figure 4.

REFERENCES

(1) Barber, J. *Chem. Soc. Rev.* **2009**, *38*, 185−196.
(2) Pace, R. In *An integrated artificial photosynthesis model*; Collings, A. F., Critchley, C., Eds.; Wiley-VCH: Weinheim, 2005.
(3) Bockris, O. M. In *Energy-The Solar Hydrogen Alternative*; Wiley & Sons: New York, 1977.
(4) Swierk, J. R.; Mallouk, T. E. *Chem. Soc. Rev.* **2013**, *42*, 2357−2387.
(5) Du, P.; Kokhan, O.; Chapman, K. W.; Chupas, P. J.; Tiede, D. M. *J. Am. Chem. Soc.* **2012**, *134*, 11096−11099.
(6) Kanan, M. W.; Nocera, D. G. *Science* **2008**, *321*, 1072−1075.
(7) Najafpour, M. M.; Barber, J.; Shen, J. R.; Moore, G.; Govindjee. *Chemistry World* **2012**, *11*, 43.
(8) Yachandra, V. K.; DeRose, V. J.; Latimer, M. J.; Mukerji, I.; Sauer, K.; Klein, M. P. *Science* **1993**, *260*, 675−679.
(9) Penner-Hahn, J. E. In *Structural characterization of the Mn site in the photosynthetic oxygen-evolving complex*; Hill, H. A. O., Sadler, P. J., Thomson, A. J., Eds.; Springer: Berlin /Heidelberg, Germany, 1998; Vol. *90*, pp 1−36.
(10) Dau, H.; Iuzzolino, L.; Dittmer, J. *Biochim. Biophys. Acta* **2001**, *1503*, 24−39.
(11) Sauer, K.; Yano, J.; Yachandra, V. K. *Coord. Chem. Rev.* **2008**, *252*, 318−335.
(12) Zouni, A.; Witt, H. T.; Kern, J.; Fromme, P.; Krauss, N.; Saenger, W.; Orth, P. *Nature* **2001**, *409*, 739−743.
(13) Kamiya, N.; Shen, J. R. *Proc. Natl. Acad. Sci. U. S. A.* **2003**, *100*, 98−103.
(14) Ferreira, K. N.; Iverson, T. M.; Maghlaoui, K.; Barber, J.; Iwata, S. *Science* **2004**, *303*, 1831−1838.
(15) Loll, B.; Kern, J.; Saenger, W.; Zouni, A.; Biesiadka, J. *Nature* **2005**, *438*, 1040−1044.
(16) Yano, J.; Kern, J.; Sauer, K.; Latimer, M. J.; Pushkar, Y.; Biesiadka, J.; Loll, B.; Saenger, W.; Messinger, J.; Zouni, A.; Yachandra, V. K. *Science* **2006**, *314*, 821−825.
(17) Murray, J. W.; Maghlaoui, K.; Kargul, J.; Ishida, N.; Lai, T. L.; Rutherford, A. W.; Sugiura, M.; Boussac, A.; Barber, J. *Energy Environ. Sci.* **2008**, *1*, 161−166.
(18) Kawakami, K.; Umena, Y.; Kamiya, N.; Shen, J. R. *Proc. Natl. Acad. Sci. U. S. A.* **2009**, *106*, 8567−8572.
(19) Guskov, A.; Kern, J.; Gabdulkhakov, A.; Broser, M.; Zouni, A.; Saenger, W. *Nat. Struct. Mol. Biol.* **2009**, *16*, 334−342.
(20) Broser, M.; Glöckner, C.; Gabdulkhakov, A.; Guskov, A.; Buchta, J.; Kern, J.; Müh, F.; Dau, H.; Saenger, W.; Zouni, A. *J. Biol. Chem.* **2011**, *286*, 15964−15972.
(21) Umena, Y.; Kawakami, K.; Shen, J. R.; Kamiya, N. *Nature* **2011**, *473*, 55−60.
(22) Allakhverdiev, S. I. *J. Photochem. Photobiol., B* **2011**, *104*, 1−8.
(23) Sproviero, E. M.; Gascón, J. A.; McEvoy, J. P.; Brudvig, G. W.; Batista, V. S. *J. Am. Chem. Soc.* **2008**, *130*, 3428−3442.
(24) Dau, H.; Zaharieva, I.; Haumann, M. *Curr. Opin. Chem. Biol.* **2012**, *16*, 3−10.
(25) Pokhrel, R.; Brudvig, G. W. In *Complex Systems: Photosynthesis*; Reedijk, J., Poeppelmeier, K., Eds.; Elsevier: Amsterdam, The Netherlands, 2013; Vol. *3*, pp 385−422.
(26) Renger, G. *Biochim. Biophys. Acta* **2001**, *1503*, 210−228.
(27) Gray, H. B. *Nat. Chem.* **2009**, *1*, 7.
(28) Armand, M.; Tarascon, J. M. *Nature* **2008**, *451*, 652−657.
(29) Yin, Q.; Tan, J. M.; Besson, C.; Geletii, Y. V.; Musaev, D. G.; Kuznetsov, A. E.; Luo, Z.; Hardcastle, K. I.; Hill, C. L. *Science* **2010**, *328*, 342−345.
(30) Lutterman, D. A.; Surendranath, Y.; Nocera, D. G. *J. Am. Chem. Soc.* **2009**, *131*, 3838−3839.
(31) Nosonovsky, M.; Bhushan, B. *Philos. Trans. R. Soc.* **2009**, *367*, 1607−1627.
(32) Amendola, V.; Meneghetti, M. *Nanoscale* **2009**, *1*, 74−88.
(33) Zheludkevich, M. L.; Ferreira, M. G. S.; Raps, D.; Hack, T. "*Self-healing anticorrosion coatings*" in "*Self-healing properties of new surface treatments*", Fedrizzi, L.; Fürbeth, W.; Montemor, F. (editors); Maney Publishing, Wakefield, 2011, Chapter 2.
(34) Ghosh, S. K. In *Self-healing Materials: Fundamentals, Design Strategies, and Applications*; Wiley-VCH: Weinheim, 2008; pp 10−30.
(35) Hill, C. L.; Zhang, X. *Nature* **1995**, *373*, 324−326.
(36) Murphy, E. B.; Wudl, F. *Prog. Polym. Sci.* **2010**, *35*, 223−251.
(37) Wool, R. P. *Soft Matter.* **2008**, *4*, 400−418.
(38) Yuan, Y. C.; Yin, T.; Rong, M. Z.; Zhang, M. Q. *Express Polym. Lett.* **2008**, *2*, 238−250.
(39) Amendola, V.; Meneghetti, M. "*Self-Healing at the Nanoscale: Mechanisms and Key Concepts of Natural and Artificial Systems*", CRC Press, Boca Raton, 2011, Chapters 1, 2 and 4.
(40) Olugebefola, S. C.; Aragon, A. M.; Hansen, C. J.; Hamilton, A. R.; Kozola, B. D.; Wu, W.; Geubelle, P. H.; Lewis, J. A.; Sottos, N. R.; White, S. R. *J. Compos. Mater.* **2010**, *44*, 2587−2603.
(41) Youngblood, J. P.; Sottos, N. R. *MRS Bull.* **2008**, *33*, 732−741.
(42) Rule, J. D.; Brown, E. N.; Sottos, N. R.; White, S. R.; Moore, J. S. *Adv. Mater.* **2005**, *17*, 205−208.
(43) Amendola, V.; Meneghetti, M. *Phys. Chem. Chem. Phys.* **2009**, *11*, 3805−3821.
(44) Potier, F.; Guinault, A.; Delalande, S.; Sanchez, C.; Ribot, F.; Rozes, L. *Polym. Chem.* **2014**, *5*, 4474−4479.
(45) Blaiszik, B. J.; Kramer, S. L. B.; Olugebefola, S. C.; Moore, J. S.; Sottos, N. R.; White, S. R. *Annu. Rev. Mater. Res.* **2010**, *40*, 179−211.
(46) Pirson, A. *Zeit Bot* **1937**, *31*, 193−267.

DOI: 10.1021/cs5015157
ACS Catal. 2015, 5, 1499−1512

(47) Dismukes, G. C.; Siderer, Y. *Proc. Natl. Acad. Sci. U. S. A.* **1981**, *78*, 274−278.
(48) Evelo, R. G.; Styring, S.; Rutherford, A. W.; Hoff, A. J. *Biochim. Biophys. Acta* **1989**, *973*, 428−442.
(49) Miller, A. F.; Brudvig, G. W. *Biochim. Biophys. Acta* **1991**, *1056*, 1−18.
(50) Pace, R. J.; Smith, P.; Bramley, R.; Stehlik, D. *Biochim. Biophys. Acta* **1991**, *1058*, 161−170.
(51) Hasegawa, K.; Ono, T.; Inoue, Y.; Kusunoki, M. *Chem. Phys. Lett.* **1999**, *300*, 9−19.
(52) Ioannidis, N.; Nugent, J. H. A.; Petrouleas, V. *Biochemistry* **2002**, *41*, 9589−9600.
(53) Olesen, K.; Andreasson, L. E. *Biochemistry* **2003**, *42*, 2025−2035.
(54) Britt, R. D.; Campbell, K. A.; Peloquin, J. M.; Gilchrist, M. L.; Aznar, C. P.; Dicus, M. M.; Robblee, J.; Messinger, J. *Biochim. Biophys. Acta* **2004**, *1655*, 158−171.
(55) Kulik, L. V.; Epel, B.; Lubitz, W.; Messinger, J. *J. Am. Chem. Soc.* **2005**, *127*, 2392−2393.
(56) Haddy, A. *Photosynth. Res.* **2007**, *92*, 357−368.
(57) Pantazis, D. A.; Orio, M.; Petrenko, T.; Zein, S.; Lubitz, W.; Messinger, J.; Neese, F. *Phys. Chem. Chem. Phys.* **2009**, *11*, 6788−6798.
(58) Teutloff, C.; Pudollek, S.; Kessen, S.; Broser, M.; Zouni, A.; Bittl, R. *Phys. Chem. Chem. Phys.* **2009**, *11*, 6715−6726.
(59) Hillier, W.; Babcock, G. T. *Biochemistry* **2001**, *40*, 1503−1509.
(60) Yamanari, T.; Kimura, Y.; Mizusawa, N.; Ishii, A.; Ono, T. A. *Biochemistry* **2004**, *43*, 7479−7490.
(61) Debus, R. J. *Coord. Chem. Rev.* **2008**, *252*, 244−258.
(62) Noguchi, T. *Coord. Chem. Rev.* **2008**, *252*, 336−346.
(63) Yachandra, V. K.; Guiles, R. D.; McDermott, A.; Britt, R. D.; Dexheimer, S. L.; Sauer, K.; Klein, M. P. *Biochim. Biophys. Acta* **1986**, *850*, 324−332.
(64) MacLachlan, D. J.; Hallahan, B. J.; Ruffle, S. V.; Nugent, J. H.; Evans, M. C.; Strange, R. W.; Hasnain, S. S. *Biochem. J.* **1992**, *285*, 569−576.
(65) Mekky Koua, F. H.; Umena, Y.; Kawakami, K.; Shen, J. R. *Proc. Natl. Acad. Sci. U. S. A.* **2013**, *110*, 3889−3894.
(66) Debus, R. J. *Biochim. Biophys. Acta* **1992**, *1102*, 269−352.
(67) Yachandra, V. K.; Sauer, K.; Klein, M. P. *Chem. Rev.* **1996**, *96*, 2927−2950.
(68) Sproviero, E. M.; Gascon, J. A.; McEvoy, J. P.; Brudvig, G. W.; Batista, V. S. *Curr. Opin. Struct. Biol.* **2007**, *17*, 173−180.
(69) Dau, H.; Dittmer, J.; Epple, M.; Hanss, J.; Kiss, E.; Rehder, D.; Schulzke, C.; Vilter, H. *FEBS Lett.* **1999**, *457*, 237−240.
(70) Rehder, D.; Schulzke, C.; Dau, H.; Meinke, C.; Hanss, J.; Epple, M. *J. Inorg. Biochem.* **2000**, *80*, 115−121.
(71) Haumann, M.; Barra, M.; Loja, P.; Loscher, S.; Krivanek, R.; Grundmeier, A.; Andreasson, L. E.; Dau, H. *Biochemistry* **2006**, *45*, 13101−13107.
(72) Aro, E. M.; Virgin, I.; Andersson, B. *Biochim. Biophys. Acta -Bioenergetics* **1993**, *1143*, 113−134.
(73) Herbstová, M.; Tietz, S.; Kinzel, C.; Turkina, M. V.; Kirchhoff, H. *Proc. Natl. Acad. Sci. U. S. A.* **2012**, *109*, 20130−20135.
(74) Kato, Y.; Sun, X.; Zhang, L.; Sakamoto, W. *Plant Physiol.* **2012**, *159*, 1428−1439.
(75) Tamura, N.; Cheniae, G. M. *Biochim. Biophys. Acta* **1987**, *890*, 179−194.
(76) Miller, A. F.; Brudvig, G. *Biochemistry* **1989**, *28*, 8181−8190.
(77) Bondarava, N.; Beyer, P.; Krieger-Liszkay, A. *Biochim. Biophys. Acta* **2005**, *1708*, 63−70.
(78) Nixon, P. J.; Diner, B. A. *Biochemistry* **1992**, *31*, 942−948.
(79) Dasgupta, J.; Ananyev, G. M.; Dismukes, G. C. *J. Coord. Chem.* **2008**, *252*, 347−360.
(80) Nowaczyk, M. M.; Hebeler, R.; Schlodder, E.; Meyer, H. E.; Warscheid, B.; Rögner, M. *Plant Cell* **2006**, *18*, 3121−3131.
(81) Becker, K.; Cormann, K. U.; Nowaczyk, M. M. *J. Photochem. Photobiol., B* **2011**, *104*, 204−211.
(82) Cheniae, G. M.; Martin, I. F. *Biochim. Biophys. Acta* **1971**, *253*, 167−181.
(83) Ananyev, G. M.; Dismukes, G. C. *Biochemistry* **1996**, *35*, 14608−14617.
(84) Ananyev, G. M.; Dismukes, G. C. *Biochemistry* **1996**, *35*, 4102−4109.
(85) Hwang, H. J.; Burnap, R. L. *Biochemistry* **2005**, *44*, 9766−9774.
(86) Zaltsman, L.; Ananyev, G. M.; Bruntrager, E.; Dismukes, G. C. *Biochemistry* **1997**, *36*, 8914−8922.
(87) Lucas, J. M. PNEUMATIC TIRE. U.S. patent 598613, 1898.
(88) Suzuki, O.; Takahashi, M.; Fukunaga, T.; Kuboyama, J. U.S. patent 3 399966, 1968.
(89) Najafpour, M. M.; Kompany-Zareh, M.; Zahraei, A.; Jafarian Sedigh, D.; Jaccard, H.; Khoshkam, M.; Britt, R. D.; Casey, W. *Dalton Trans.* **2013**, *42*, 14603−14611.
(90) Huynh, M.; Bediako, D. K.; Nocera, D. G. *J. Am. Chem. Soc.* **2014**, *136*, 6002−6010.
(91) Najafpour, M. M.; Jafarian Sedigh, D.; Pashaei, B.; Nayeri, S. *New J. Chem.* **2013**, *37*, 2448−2459.
(92) Glikman, T. S.; Shcheglova, I. S. *Kinetika i Kataliz.* **1968**, *9*, 461−470.
(93) Jiang, S. P.; Chen, Y. Z.; You, J. K.; Chen, T. X.; Tseung, A. C. C. *J. Electrochem. Soc.* **1990**, *137*, 3374−3380.
(94) Jiang, S. P.; Tseung, A. C. C. *J. Electrochem. Soc.* **1991**, *138*, 1216−1222.
(95) McAlpin, J. G.; Surendranath, Y.; Dinca, M.; Stich, T. A.; Stoian, S. A.; Casey, W. H.; Nocera, D. G.; Britt, R. D. *J. Am. Chem. Soc.* **2010**, *132*, 6882−6883.
(96) Esswein, A. J.; Surendranath, Y.; Reece, S. Y.; Nocera, D. G. *Energy Environ. Sci.* **2011**, *4*, 499−504.
(97) Surendranath, Y.; Lutterman, D. A.; Liu, Y.; Nocera, D. G. *J. Am. Chem. Soc.* **2012**, *134*, 6326−6336.
(98) (a) Risch, M.; Khare, V.; Zaharieva, I.; Gerencser, L.; Chernev, P.; Dau, H. *J. Am. Chem. Soc.* **2009**, *131*, 6936−6937. (b) Du, P.; Kokhan, O.; Chapman, K. W.; Chupas, P. J.; Tiede, D. M. *J. Am. Chem. Soc.* **2012**, *134*, 11096−11099.
(99) Surendranath, Y.; Kanan, M. W.; Nocera, D. G. *J. Am. Chem. Soc.* **2010**, *132*, 16501−16509.
(100) Kanan, M. W.; Yano, J.; Surendranath, Y.; Dincă, M.; Yachandra, V. K.; Nocera, D. G. *J. Am. Chem. Soc.* **2010**, *132*, 13692−13701.
(101) Gerken, J. B.; McAlpin, J. G.; Chen, J. Y. C.; Rigsby, M. L.; Casey, W. H.; Britt, R. D.; Stahl, S. S. *J. Am. Chem. Soc.* **2011**, *133*, 14431−14442.
(102) Rosen, J.; Hutchings, G. S.; Jiao, F. *J. Am. Chem. Soc.* **2013**, *135*, 4516−4521.
(103) Grewe, T.; Deng, X.; Tüysüz, H. *Chem. Mater.* **2014**, *26*, 3162−3168.
(104) Han, A.; Wu, H.; Sun, Z.; Jia, H.; Du, P. *Phys. Chem. Chem. Phys.* **2013**, *15*, 12534−12538.
(105) Fihri, A.; Artero, V.; Razavet, M.; Baffert, C.; Leibl, W.; Fontecave, M. *Angew. Chem., Int. Ed.* **2008**, *47*, 564−567.
(106) Halpert, G. *J. Power Sources* **1984**, *12*, 177−192.
(107) Merrill, M. D.; Dougherty, R. C. *J. Phys. Chem. C* **2008**, *112*, 3655−3666.
(108) Garche, J., In *Encyclopedia of Electrochemical Power Sources*; Elsevier, 2009.
(109) Appleby, A. J.; Crepy, G.; Jacquelin. *J. Int. J. Hydrogen Energy* **1978**, *3*, 21−37.
(110) Hall, D. E. J. *Electrochem. Soc.* **1983**, *130*, 317−321.
(111) Singh, R. N.; Bahadur, L.; Pandey, J. P.; Singh, S. P.; Chartier, P.; Poillerat, G. *J. Appl. Electrochem.* **1994**, *24*, 149−156.
(112) Suredini, H. B.; Cerne, J. L.; Crnkovic, F. C.; Machado, S. A. S.; Avaca, L. A. *Int. J. Hydrogen Energy* **2000**, *25*, 415−423.
(113) Lu, P. W. T.; Srinivasan, S. *J. Electrochem. Soc.* **1978**, *125*, 1416−1422.
(114) Corrigan, D. A. *J. Electrochem. Soc.* **1987**, *134*, 377−384.
(115) Li, X.; Walsh, F. C.; Pletcher, D. *Phys. Chem. Chem. Phys.* **2011**, *13*, 1162−1167.
(116) Dinca, M.; Surendranath, Y.; Nocera, D. G. *Proc. Natl. Acad. Sci. U. S. A.* **2010**, *107*, 10337−10341.
(117) Singh, A.; Chang, S. L. Y.; Hocking, R. K.; Bach, U.; Spiccia, L. *Energy Environ.Sci.* **2013**, *6*, 579−586.

DOI: 10.1021/cs5015157
ACS Catal. 2015, 5, 1499−1512

(118) Singh, A.; Chang, S. L. Y.; Bach, U.; Spiccia, L. *Catal. Sci. Technol.* **2013**, *3*, 1725−1732.
(119) Pourbaix, M. *Atlas of Electrochemical Equilibria in Aqueous Solutions*; Pergamon, 1966.
(120) Gao, M.; Sheng, W.; Zhuang, Z.; Fang, Q.; Gu, S.; Jiang, J.; Yan, Y. *J. Am. Chem. Soc.* **2014**, *136* (19), 7077−7084.
(121) Morita, M.; Iwakura, C.; Tamura, H. *Electrochim. Acta* **1977**, *22*, 325−328.
(122) Morita, M.; Iwakura, C.; Tamura, H. *Electrochim. Acta* **1979**, *24*, 357−362.
(123) Shafirovich, V. Y.; Khannanov, N. K.; Shilov, A. E. *J. Inorg. Biochem.* **1981**, *15*, 113−129.
(124) Luneva, N. P.; Knerelman, E. I.; Shafirovich, V. Y.; Shilov, A. E. *J. Chem. Soc. Chem. Commun.* **1987**, 1504−1505.
(125) Dismukes, G. C.; Brimblecombe, R.; Felton, G. A. N.; Pryadun, R. S.; Sheats, J. E.; Spiccia, L.; Swiegers, G. F. *Acc. Chem. Res.* **2009**, *42*, 1935−1943.
(126) Najafpour, M. M.; Ehrenberg, T.; Wiechen, M.; Kurz, P. *Angew. Chem., Int. Ed.* **2010**, *49*, 2233−2237.
(127) Wiechen, M.; Berends, H. M.; Kurz, P. *Dalton Trans.* **2012**, *41*, 21−31.
(128) Iyer, A.; Del-Pilar, J.; King'ondu, C. K.; Kissel, E.; Garces, H. F.; Huang, H.; El-Sawy, A. M.; Dutta, P. K.; Suib, S. L. *J. Phys. Chem. C* **2012**, *116*, 6474−6483.
(129) Najafpour, M. M.; Jafarian Sedigh, D. *Dalton Trans.* **2013**, *42*, 12173−12178.
(130) Najafpour, M. M.; Haghighi, B.; Jafarian Sedigh, D.; Zarei Ghobadi, M. *Dalton Trans.* **2013**, *42*, 16683−16686.
(131) Yagi, M.; Kaneko, M. *Chem. Rev.* **2001**, *101*, 21−35.
(132) Manchanda, R.; Brudvig, G. W.; Crabtree, R. H. *Coord. Chem. Rev.* **1995**, *144*, 1−38.
(133) Brimblecombe, R.; Koo, A.; Dismukes, G. C.; Swiegers, G. F.; Spiccia, L. *J. Am. Chem. Soc.* **2010**, *132*, 2892−2894.
(134) Brimblecombe, R.; Koo, A.; Dismukes, G. C.; Swiegers, G. F.; Spiccia, L. *ChemSusChem* **2010**, *3*, 1146−1150.
(135) Hocking, R. K.; Brimblecombe, R.; Chang, L.; Singh, A.; Cheah, M. H.; Glover, C.; Casey, W. H.; Spiccia, L. *Nat. Chem.* **2011**, *3*, 461−466.
(136) Izgorodin, A.; Winther-Jensen, O.; Macfarlane, D. R. *Aust. J. Chem.* **2012**, *65*, 638−642.
(137) Singh, A.; Hocking, R. K.; Chang, L. Y.; George, B. M.; Fehr, M.; Lips, K.; Schnegg, A.; Spiccia, L. *Chem. Mater.* **2013**, *25*, 1098−1108.
(138) Chang, S. L. Y.; Singh, A.; Hocking, R. K.; Dwyer, C.; Spiccia, L. *J. Mater. Chem. A* **2014**, *2*, 3730−3733.
(139) Khan, M.; Suljoti, E.; Singh, A.; Bonke, S.; Brandenburg, T.; Yamamoto, K.; Atak, K.; Golnak, R.; Spiccia, L.; Aziz, E. F. *J. Mater. Chem. A* **2014**, *2*, 18199−18203.
(140) Urban, M. W. *Nat. Chem.* **2012**, *4*, 80−82.

DOI: 10.1021/cs5015157
ACS Catal. 2015, 5, 1499−1512